Electrical Properties and Sinterability for Lithium Germanium Phosphate $Li_{1+x}M_xGe_{2-x}(PO_4)_3$, M=Al, Cr, Ga, Fe, Sc, and In Systems

Hiromichi Aono, Eisuke Sugimoto, Yoshihiko Sadaoka,†
Nobuhito Imanaka,††* and Gin-ya Adachi,*,††
Department of Industrial Chemistry, Niihama National College of Technology,
7-1 Yagumo-cho, Niihama, Ehime 792
†Department of Applied Chemistry, Faculty of Engineering, Ehime University,
3 Bunkyo-cho, Matsuyama, Ehime 790
††Department of Applied Chemistry, Faculty of Engineering, Osaka University,
2-1 Yamadaoka, Suita, Osaka 565
(Received March 13, 1992)

The electrical properties and sinterability were studied for $Li_{1+x}M_xGe_{2-x}(PO_4)_3$, M=$Al^{3+}$, Cr^{3+}, Ga^{3+}, Fe^{3+}, Sc^{3+}, and In^{3+} systems. Due to the closer ionic radius of Al^{3+} and Cr^{3+} compared to that of Ge^{4+}, those M^{3+} ions easily substitute the Ge^{4+} site. Larger cations, such as Ga^{3+}, Fe^{3+}, Sc^{3+}, and In^{3+}, were difficult to substitute the Ge^{4+} site. The ionic conductivity and sinterability improved with an increase in x for all of the M^{3+}-substituted systems. In particular, an Al^{3+}- or Cr^{3+}-substituted system shows higher conductivity; the maximum conductivity is 2.4×10^{-4} S cm^{-1} at 298 K for $Li_{1.5}Al_{0.5}Ge_{1.5}(PO_4)_3$. The enhancement in the conductivity is attributed to a decrease in the porosity and a lowering of the activation energy in the grain boundaries. The activation energy for Li^+ ion conduction of the bulk component was 0.38 eV for $Li_{1+x}M_xGe_{2-x}(PO_4)_3$ electrolytes, and was almost independent of M^{3+} substitution.

A lithium solid electrolyte has been extensively investigated for the application to high-energy density, long-life batteries. In particular, highly conducting lithium at room temperature is a promising electrolyte for this purpose, owing to its light weight and high electrochemical potential.[1,2]

Recently, solid electrolytes based on $LiTi_2(PO_4)_3$, $Li_{1+x}M_xTi_{2-x}(PO_4)_3$, M=Al, Sc, Y, or La, etc. system,[3-10] or $LiTi_2(PO_4)_3$+lithium salt system,[11,12] have been reported to show high conductivity, even at room temperature. Although $LiTi_2(PO_4)_3$ shows poor conductivity, it could be greatly enhanced by M^{3+} substitution or the addition of a lithium salt, such as Li_3PO_4 or Li_3BO_3. $LiM_2(PO_4)_3$, where M^{4+} are Ge,[13] Hf,[5,14] and Zr,[14,15] are the analogue electrolyte. However, the conductivity for these phosphates is considerably low compared with those for the $LiTi_2(PO_4)_3$ series. $LiTi_2(PO_4)_3$ is supposed to form the best host structure, since the tunnel size in the phosphate is suitable for Li^+ ion migration. The lattice constants for $LiGe_2(PO_4)_3$ are smaller than those for $LiTi_2(PO_4)_3$. If the Ge^{4+} site is partially substituted by a larger M^{3+} ion, the tunnel size may be expected to approach that of $LiTi_2(PO_4)_3$. Although Li et al. have reported that the conductivity increases with the value of x for the $Li_{1+x}M_xGe_{2-x}(PO_4)_3$, M=Al (0.535 Å) and Cr (0.615 Å) systems,[13] whose ionic radii[16] are close to that of Ge^{4+} (0.530 Å), no other cation has been tried regarding substitution.

In the present work, we tried to increase the lattice size for $LiGe_2(PO_4)_3$ by a larger M^{3+} ion substitution to the Ge^{4+} site in order to achieve higher conductivity, even at room temperature, and clarified the electrical properties for the bulk and grain boundary.

Experimental

1. Materials. Li_2CO_3 (purity: 99.99%), GeO_2 (99.999%), $(NH_4)_2HPO_4$ (extra pure grade), and M_2O_3 M=Al, Cr, Ga, Fe, Sc, In (99.99%) were used as starting materials. The mixture was reacted in a platinum crucible at 1173 K for 2 h in an air atmosphere. The resulting material was ground into fine powder using a ball-mill for 6 h through a wet process (methanol). The dried powder was again heated at 1173 K for 2 h; it was then ball-milled for 12 h by the same process. The particle size of the dried powder was smaller than 1 μm, which was determined by a centrifugal particle size analyzer (Shimadzu SA-CP3). The powder was pressed into a pellet at a pressure of 1×10^8 Pa. It was then sintered at 1073—1273 K for 2 h in an air atmosphere. Both surfaces of the sintered pellet were polished and gold electrodes were sputtered by an Ion Coater (Shimadzu IC-50).

2. Measurement. An X-ray powder diffraction analysis was conducted using a Rigaku Rotaflex with high-purity Si powder (99.99%) as an internal standard. The ionic conductivity for the bulk and grain boundary was determined by a complex impedance method[17] using an LCZ meter (4276A, 4277A from Hewlett Packard Co., Ltd.). The porosity of the sintered pellets was measured by the Archimedes' method.

Results and Discussion

1. Phases. $LiGe_2(PO_4)_3$ has a NASICON-type[18,19] three-dimensional network structure. Both GeO_6 octahedra and PO_4 tetrahedra in $LiGe_2(PO_4)_3$ are linked by their corners to form a three-dimensional network with the space group $R\bar{3}c$.[20] Two different lithium-ion sites, (A(1) and A(2)) exist in the phosphate. For $LiGe_2(PO_4)_3$, Li^+ ions fully occupy the A(1) sites, but are vacant in the A(2) site. The occupation degree of the A(2) sites by Li^+ increases with an increase in x for the $Li_{1+x}M_xGe_{2-x}(PO_4)_3$ system.

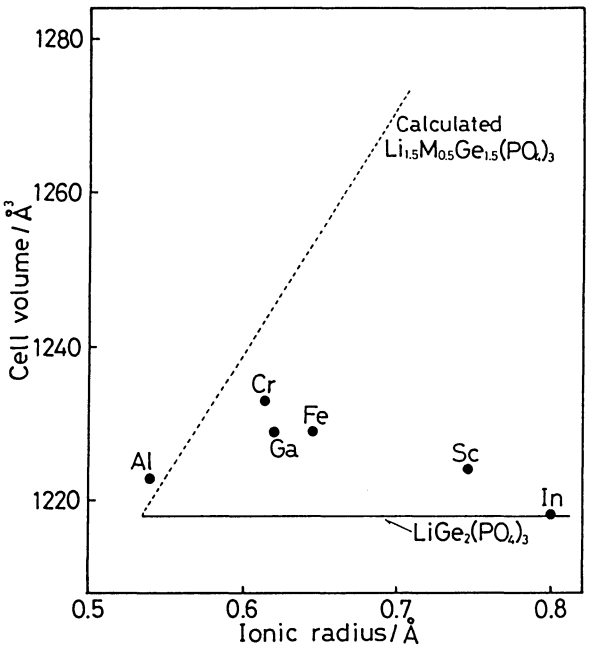

Fig. 1. Relationship between the M^{3+} ionic radius and the cell volume for $Li_{1.5}M_{0.5}Ge_{1.5}(PO_4)_3$.

Figure 1 shows the relationship between the ionic radius of the M^{3+} ion and the cell volume for $Li_{1.5}M_{0.5}Ge_{1.5}(PO_4)_3$. The cell volume was estimated from the lattice constants obtained by the X-ray powder diffraction method. The broken line corresponds to the cell volume calculated based on the assumption that the M^{3+} ion completely substitutes the Ge^{4+} site. Figure 2 presents the X-ray diffraction patterns for samples of $Li_{1.5}M_{0.5}Ge_{1.5}(PO_4)_3$, M=Al, Cr, Ga, Fe, Sc, In. The $LiGe_2(PO_4)_3$ pattern is also shown as a reference. For the Al^{3+} and Cr^{3+} systems, the cell volume is close to the calculated value; only the $R\bar{3}c$ phase has been confirmed by X-ray diffraction analyses. The Al^{3+} and Cr^{3+} ions easily substitute the Ge^{4+} site, since these M^{3+} ions are close to Ge^{4+} regarding the ionic radius. The tunnel size increases, if the Ge^{4+} site is substituted by a larger M^{3+} ion. We expected that the cell volume would increase upon substitution of the Ge^{4+} site by larger M^{3+} ions, such as Fe^{3+} or Sc^{3+}. However, the obtained cell volume is lower than the calculated one. This cell volume did not increase if the sintering temperature was raised. The Ge^{4+} ion in $LiGe_2(PO_4)_3$ can not be easily substituted by a larger M^{3+} ion. The cell volume for the In^{3+} system is the same for that of $LiGe_2(PO_4)_3$. This indicates that no replacement occurs for the larger In^{3+} system. On the other hand, some unknown peaks were also observed for the Ga^{3+}, Fe^{3+}, Sc^{3+}, In^{3+} systems. The number of the unknown peaks and the intensity of these peaks increase with an enlargement in the ionic radius of the M^{3+} ion. The second phase would be obtained, since the replacement of the Ge^{4+} site is difficult for these larger M^{3+} ions. These unknown peaks were not assigned to the $Li_3M_2(PO_4)_3$ phase, M=Ga, Fe, Sc, In.

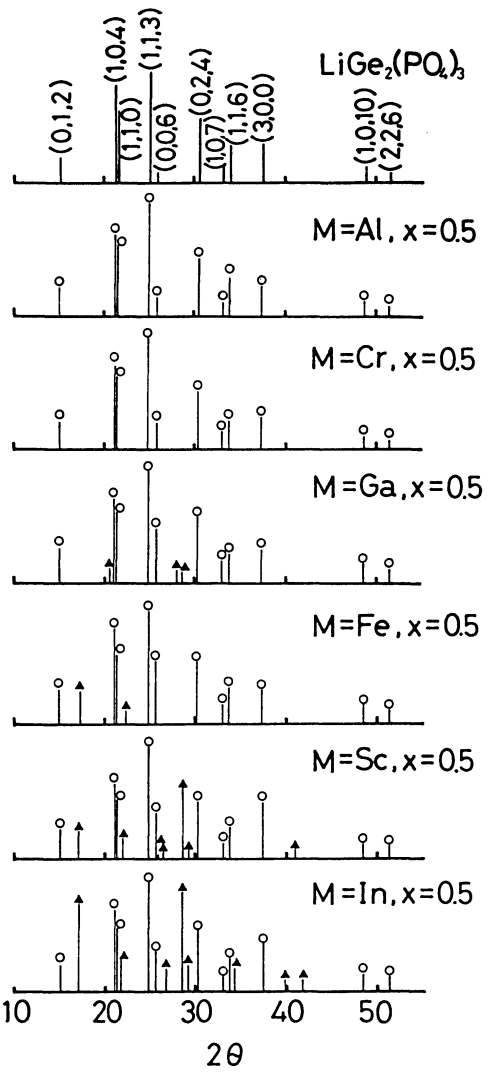

Fig. 2. X-Ray diffraction patterns (Cu $K\alpha$) for $LiGe_2(PO_4)_3$ and $Li_{1.5}M_{0.5}Ge_{1.5}(PO_4)_3$, M=Al, Cr, Ga, Fe, Sc, In. $R\bar{3}c$ phase (○), unknown phase (▲).

2. Conductivity and Sinterability. Figure 3 shows the relationship between the conductivity and x for the $Li_{1+x}M_xGe_{2-x}(PO_4)_3$ systems at 298 K. The conductivity is greatly enhanced along with the increase in x for all of the systems examined. In particular, the conductivity for the Al^{3+} and Cr^{3+} systems is higher than that for the other systems. A maximum conductivity of 2.4×10^{-4} S cm^{-1} was obtained for $Li_{1.5}Al_{0.5}Ge_{1.5}(PO_4)_3$, which is about one order of magnitude higher than that reported by Li et al.[13] In this study, the particle size of the ball-milled powders before sintering was smaller than 1 μm. However, the well-ground process was not described in the paper of Li et al. The difference in the grinding process would influence both the conductivity and sinterability. By substituting a larger M^{3+} ion, the conductivity became lower, compared with that for smaller M^{3+} (Al^{3+} or Cr^{3+}) systems. A poorly conductive second phase might be formed, which would

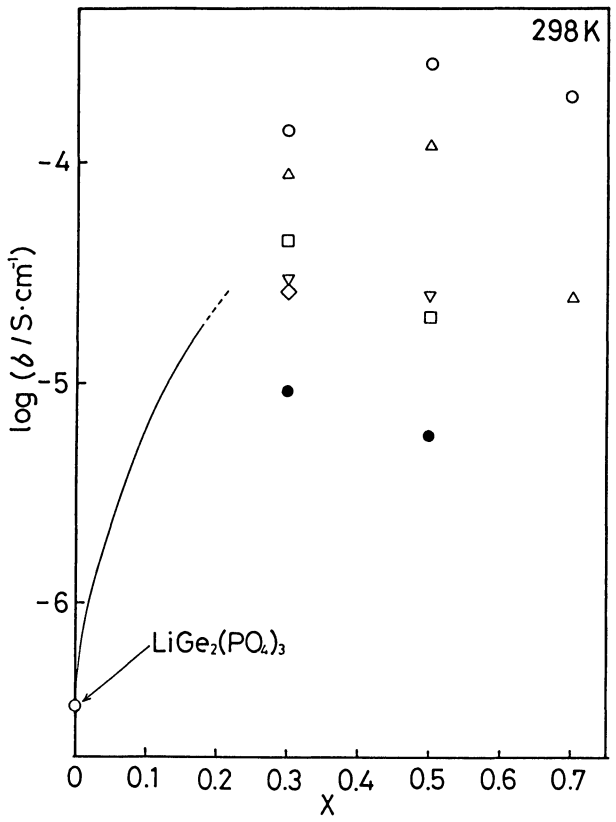

Fig. 3. Conductivity at 298 K vs. the x value for the $Li_{1+x}M_xGe_{2-x}(PO_4)_3$ systems. M=Al (○), Cr (△), Ga (□), Fe (▽), Sc (◇), In (●).

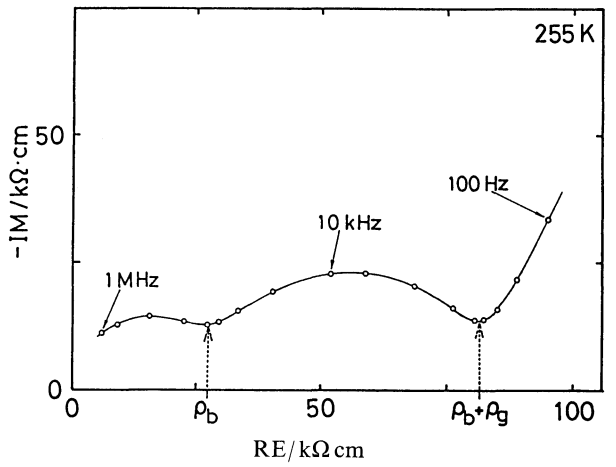

Fig. 4. Complex impedance plot for $Li_{1.5}Al_{0.5}Ge_{1.5}(PO_4)_3$ at 255 K.

block Li^+ migration at the grain boundaries.

Figure 4 shows a representive complex impedance plot (Cole–Cole plot) of $Li_{1.5}Al_{0.5}Ge_{1.5}(PO_4)_3$. Two semicircles were observed.[21] The bulk and the total resistances were determined from these semicircles, as is shown in the figure. The interface resistivity between the electrode and the electrolyte was also observed in a lower frequency region at higher temperatures. From these results, the conductivity for the bulk and the grain

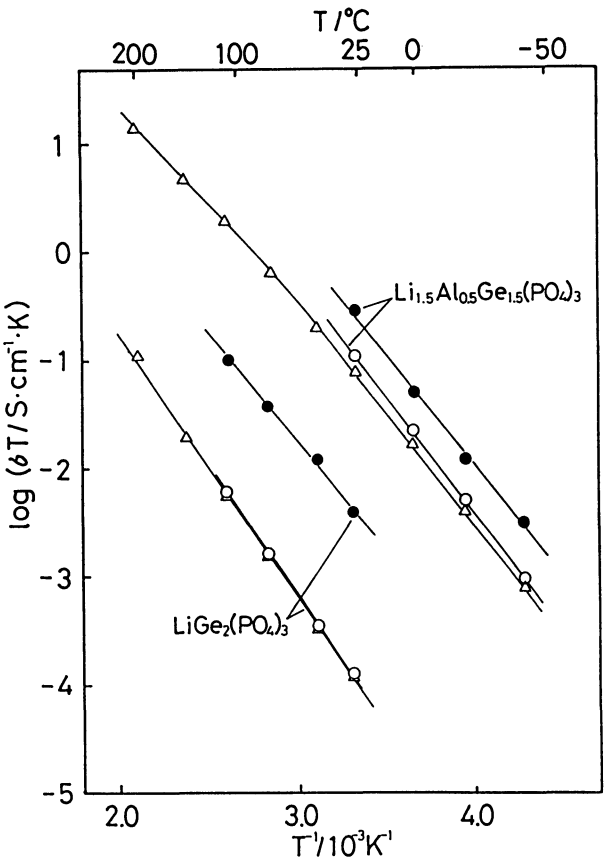

Fig. 5. Temperature dependencies of the conductivity for the bulk and the grain boundary for $LiGe_2(PO_4)_3$ and $Li_{1.5}Al_{0.5}Ge_{1.5}(PO_4)_3$. Bulk (●), grain boundary (○), total (△).

boundary can be determined. Figure 5 gives the conductivity for the bulk and the grain boundary as well as their total, for typical samples. The conductivity for the bulk is higher than that for the grain boundary. The total conductivity is almost the same as the grain boundary value. This means that the total conductivity is mainly determined by that of the grain boundaries.

The activation energies for Li^+ migration in the bulk and the grain boundary (estimated from Fig. 5) are presented in Fig. 6. The activation energy for the bulk and the grain boundary can not be determined for a higher x region, or for Sc^{3+} and In^{3+} substituted systems, since the two clear semicircles were not obtained on the complex impedance plane. Regarding the bulk component, the activation energy does not change upon M^{3+} substitution. The change in the lattice size and lithium insertion in the A(2) site by M^{3+} substitution do not influence Li^+ conduction in the 3D network structure. The activation energy for Li^+ migration in bulk for the $LiGe_2(PO_4)_3$ structure is 0.38 eV. This is higher than that for the $LiTi_2(PO_4)_3$ structure of 0.30 eV.[10,12] The cell volume for $LiTi_2(PO_4)_3$ is 1307 Å^3, which is larger than 1218—1230 Å^3 for the Ge-systems. The small lattice size for $LiGe_2(PO_4)_3$ makes the activation energy increase for Li^+ migration in the 3D network

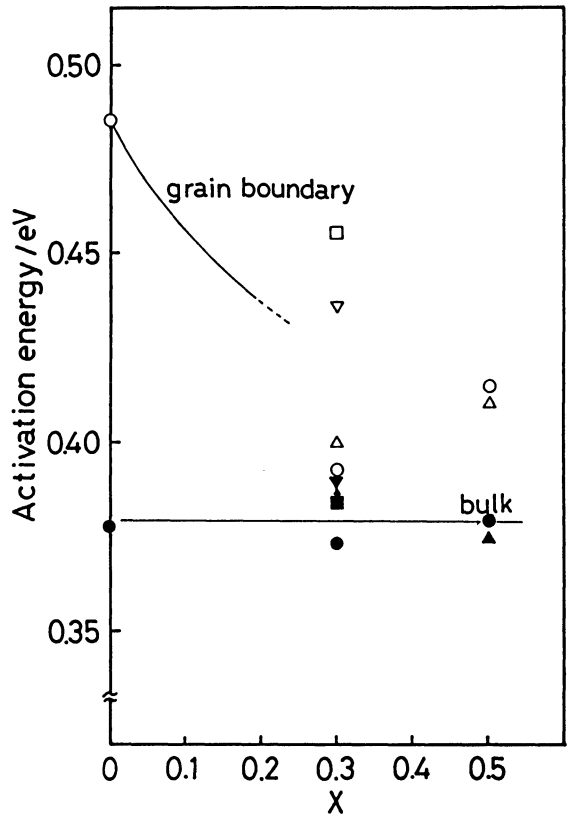

Fig. 6. Activation energy for the bulk and the grain boundary in $Li_{1+x}M_xGe_{2-x}(PO_4)_3$ systems. M=Al: bulk (●), grain boundary (○), Cr: bulk (▲), grain boundary (△), Ga: bulk (■), grain boundary (□), Fe: bulk (▼), grain boundary (▽).

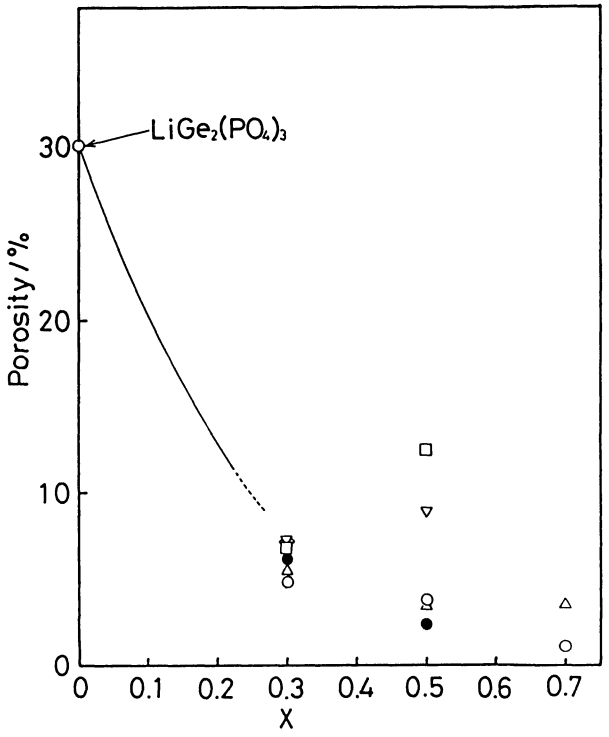

Fig. 7. Variation of the porosity for $Li_{1+x}M_xGe_{2-x}(PO_4)_3$ systems. M=Al (○), Cr (△), Ga (□), Fe (▽), Sc (◇), In (●).

structure. The activation energy for the grain boundary decreases with an increase in x.

The dependence of the porosity of the sintered pellet on x is shown in Fig. 7. No treatment could produce a dense pellet for $LiGe_2(PO_4)_3$, itself. The porosity decreased with an increase in x for all of the systems examined. This tendency is consistent with the conductivity enhancement shown in Fig. 3. The conductivity also increased for the In^{3+} system, though the ion could not be replaced with the Ge^{4+} site. One of the reasons for the conductivity enhancement is ascribed to an increase in densification. Although the porosity at x=0.3 was almost the same for all of the M^{3+} substitution systems, the total conductivity tends to decrease with an increase in the ionic radius of the M^{3+} ion. For the larger M^{3+} substitution samples, the activation energy for the grain boundary shows a higher value in Fig. 6. This indicates that the conductivity depends on the activation energy for the grain boundary. In our preceding paper, the reason for the conductivity enhancement with an x increase for the Ti-system of $Li_{1+x}M_xTi_{2-x}(PO_4)_3$, has been attributed to an increase in the sinterability, as well as to a decrease in the activation energy for the grain boundary.[10,22] For the Ge-system, the same explanation holds for the conductivity enhancement. The Li^+ ion conduction of the grain boundary is assimilated to that of the bulk structure by high sinterability for the x increased samples.

In conclusion, the cell volume obtained experimentally is lower than the calculated one for $Li_{1+x}M_xGe_{2-x}(PO_4)_3$, M=$Ga^{3+}$, Fe^{3+}, Sc^{3+}, and In^{3+} because these larger M^{3+} ions can not easily substitute the Ge^{4+} ions. The Al^{3+} or Cr^{3+} ion could substitute the Ge^{4+} site more easily, owing to the closer ionic radius. The conductivity is enhanced with an increase in x for all of the $Li_{1+x}M_xGe_{2-x}(PO_4)_3$ systems examined. The higher conductivity was obtained for Al^{3+}- and Cr^{3+}-substituted systems; the maximum conductivity was 2.4×10^{-4} S cm^{-1} at 298 K for $Li_{1.5}Al_{0.5}Ge_{1.5}(PO_4)_3$. The conductivity in the present systems is considerably higher than that of the other usual Li^+ conductive oxide solid electrolytes. The reason for this enhancement is attributed to an increase in the sinterability and a decrease in the activation energy at the grain boundary. The activation energy (0.38 eV) for Li^+ migration was determined for the $LiGe_2(PO_4)_3$ 3D network structure.

References

1) C. C. Liang, A. V. Joshi, and N. E. Hamilton, *J. Appl. Electrochem.*, **8**, 445 (1978).

2) K. Kanehori, K. Matsumoto, K. Miyauchi, and T. Kudo, *Solid State Ionics*, **9/10**, 1445 (1983).

3) S-ch. Li and Z-x. Lin, *Solid State Ionics*, **9/10**, 835 (1983).

4) Z-x. Lin, H-j. Yu, S-ch. Li, and S-b. Tian, *Solid State Ionics,* **18**/**19**, 549 (1986).
5) M. A. Subramanian, R. Subramanian, and A. Clearfield, *Solid State Ionics,* **18**/**19**, 562 (1986).
6) S. Hamdoune and D. Tranqui, *Solid State Ionics,* **18**/**19**, 587 (1986).
7) Z-x. Lin, H-j. Yu, S-ch. Li, and S-b. Tian, *Solid State Ionics,* **31**, 91 (1988).
8) H. Aono, E. Sugimoto, Y. Sadaoka, N. Imanaka, and G. Adachi, *J. Electrochem. Soc.,* **136**, 590 (1989).
9) H. Aono, E. Sugimoto, Y. Sadaoka, N. Imanaka, and G. Adachi, *J. Electrochem. Soc.,* **137**, 1023 (1990).
10) H. Aono, E. Sugimoto, Y. Sadaoka, N. Imanaka, and G. Adachi, *Chem. Lett.,* **1990**, 1825.
11) H. Aono, E. Sugimoto, Y. Sadaoka, N. Imanaka, and G. Adachi, *Chem. Lett.,* **1990**, 331.
12) H. Aono, E. Sugimoto, Y. Sadaoka, N. Imanaka, and G. Adachi, *Solid State Ionics,* **47**, 257 (1991).
13) S-ch. Li, J-y. Cai, and Z-x. Lin, *Solid State Ionics,* **28**—**30**, 1265 (1988).
14) B. E. Taylor, A. D. English, and T. Berzins, *Mater. Res. Bull.,* **12**, 171 (1977).
15) D. Petit, Ph. Colomban, G. Collin, and J. P. Boilot, *Mater. Res. Bull.,* **21**, 365 (1986).
16) R. D. Shannon, *Acta Crystallogr., Sect. A,* **32**, 751 (1976).
17) J. E. Bauerle, *J. Phys. Chem. Solids,* **30**, 2657 (1969).
18) H.Y-P. Hong, *Mater. Res. Bull.,* **11**, 173 (1976).
19) J. B. Goodenough, H.Y-P. Hong, and J.A. Kafalas, *Mater. Res. Bull.,* **11**, 203 (1976).
20) L. Hagman and P. Kierkegaard, *Acta Chem. Scand.,* **22**, 1882 (1968).
21) P. G. Bruce and A. R. West, *J. Electrochem. Soc.,* **130**, 662 (1983).
22) H. Aono, E. Sugimoto, Y. Sadaoka, N. Imanaka, and G. Adachi, *J. Am. Ceram. Soc.,* in contribution.